

N73-19701  
NASA CR 130924

NATIONAL AERONAUTICS AND SPACE ADMINISTRATION

*Technical Memorandum 33-596*

*Ionization Processes in Mercury Discharges*

*Frank T. Wu*

CASE FILE  
COPY

**JET PROPULSION LABORATORY  
CALIFORNIA INSTITUTE OF TECHNOLOGY  
PASADENA, CALIFORNIA**

March 1, 1973

NATIONAL AERONAUTICS AND SPACE ADMINISTRATION

*Technical Memorandum 33-596*

*Ionization Processes in Mercury Discharges*

*Frank T. Wu*

**JET PROPULSION LABORATORY  
CALIFORNIA INSTITUTE OF TECHNOLOGY  
PASADENA, CALIFORNIA**

March 1, 1973

## PREFACE

The work described in this report was performed by the Propulsion Division of the Jet Propulsion Laboratory.

## ACKNOWLEDGMENTS

The author wishes to express his appreciation to Raymond Goldstein and Che Jen Chen for their suggestions and helpful discussions and to Eugene Pawlik and Daniel Kerrisk for their interest and encouragement.

## CONTENTS

I.	Introduction . . . . .	1
II.	Single Ionization Processes . . . . .	1
	A. Direct Electron Ionization . . . . .	1
	B. Electron Impact Ionization of Excited Mercury Atoms . . . . .	3
	C. Ionization Due to Excited-State Atom Collisions . . . . .	5
III.	Double-Ionization Processes . . . . .	6
	A. Direct Neutral Ground-State Ionization by Electron Impact . . . . .	6
	B. Ionization From a Singly Ionized Ion . . . . .	8
IV.	Results and Discussion . . . . .	10
	References . . . . .	16

### FIGURES

1.	Direct electron ionization cross sections . . . . .	17
2.	Energy diagram of the mercury atom . . . . .	18
3.	Ionization cross sections for the 6P-state by electron impact . . . . .	19
4.	Direct double ionization cross sections by electron impact . . . . .	20
5.	Singly and doubly collisional ionization coefficients . . . . .	21
6.	Collisional ionization coefficients of the 6P-state by electron impact . . . . .	22
7a.	Population density $n(6P)$ vs $n_e$ for $T_e = 0.5, 1.5, 2.5,$ and $5.5$ eV at $n_a = 10^{16} \text{ cm}^{-3}$ , $g = 0$ . . . . .	23
7b.	Population density $n(6P)$ vs $T_e$ for different degrees of ionization at $n_a = 10^{16} \text{ cm}^{-3}$ , $g = 0$ . . . . .	24
8a.	Ion production rate at $n_a = 10^{16} \text{ cm}^{-3}$ , $\alpha = 10^{-1}$ . . . . .	25
8b.	Ion production rate at $n_a = 10^{16} \text{ cm}^{-3}$ , $\alpha = 10^{-2}$ . . . . .	26
8c.	Ion production rate at $n_a = 10^{16} \text{ cm}^{-3}$ , $\alpha = 10^{-3}$ . . . . .	27

CONTENTS (contd)

FIGURES (contd)

8d.	Ion production rate at $n_a = 10^{16} \text{ cm}^{-3}$ , $\alpha = 10^{-5}$ . . . . .	28
9.	Double ion production rate at $n_a = 10^{16} \text{ cm}^{-3}$ , $\alpha = 10^{-1}$ . . . . .	29
10.	Dependence of $n(6P)$ on $g$ -value for different degrees of ionization at $n_a = 10^{16} \text{ cm}^{-3}$ , $T_e = 1.5 \text{ eV}$ . . . . .	30

## ABSTRACT

This report presents a summary of theoretical calculations of the ionization processes in mercury plasma. Various possible ionization processes are analyzed and discussed. It is found that the ionization due to excited-state interactions is dominant when the degree of ionization is small and that the ionization due to multistep electron impact is significant when the degree of ionization is high.

## I. INTRODUCTION

In early studies of mercury discharge, it was believed that ionization is due mainly to the direct impact of electrons on the ground-state atoms. However, later studies have revealed that ionization can also be caused by electron impact on the excited mercury atoms. More recent work on the noble gas discharges shows that ionization due to excited state interactions is quite possible. The purpose of this study is to investigate the ionization processes in mercury plasma under various discharge conditions. The investigation was carried out in connection with the studies of Ref. 1.

## II. SINGLE IONIZATION PROCESSES

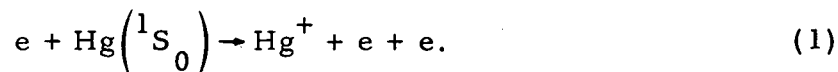
The ionization in mercury discharge is considered to be due mainly to:

- (1) Direct electron ionization.
- (2) Electron impact ionization of excited mercury atoms.
- (3) Ionization due to excited atom-atom collisions.

The analyses that follow will assume the electron distribution to be Maxwellian at temperature  $T_e$ .

### A. Direct Electron Ionization

This process can be expressed as



Although the mean electron energy is usually far lower than the threshold energy needed to ionize the mercury atom, the high-energy (or Maxwellian) tail of the electron energy distribution function is sufficient to produce the

ionization. The rate of ionization from the ground state due to electron impact can be calculated by the equation

$$Z_{1C} = n_e n \left( {}^1S_0 \right) \int_{\epsilon_{th}}^{\infty} v(\epsilon) \epsilon^{1/2} f(\epsilon) Q_{1C}(\epsilon) d\epsilon, \quad (2)$$

where  $n_e$  and  $n \left( {}^1S_0 \right)$  are the electron and the ground-state densities, respectively,  $f(\epsilon)$  is the electron energy distribution,  $\epsilon$  is the electron energy, the subscript th stands for threshold, and  $Q_{1C}(\epsilon)$  is the energy-dependent ionization cross section. The electron energy distribution  $f(\epsilon)$  is subject to the normalization condition

$$\int_0^{\infty} \epsilon^{1/2} f(\epsilon) d\epsilon = 1. \quad (3)$$

The direct ionization cross section  $Q_{1C}(\epsilon)$  can be analytically approximated using Gryzinski's formula (Refs. 2, 3):

$$Q_{1C}(\epsilon) = \frac{\sigma_0}{V_i^2} \left( \frac{V_i}{\epsilon} \right) \left( \frac{\epsilon - V_i}{\epsilon + V_i} \right)^{3/2} \times \left\{ 1 + \frac{2}{3} \left( 1 - \frac{V_i}{2\epsilon} \right) \ln \left[ 2.7 + \left( \frac{\epsilon - V_i}{V_i} \right)^{1/2} \right] \right\} \quad (4)$$

$$\sigma_0 = 2 \times 6.56 \times 10^{-4} \text{ cm}^2 - \text{ev}^2,$$

where  $\epsilon$  is the incident kinetic energy of the electron in electron volts, and  $V_i$  is the ionization threshold energy and is equal to 10.43 eV.

The cross section thus calculated from Eq. (4) is shown in Fig. 1, which also presents the experimentally available ionization cross sections for comparison. Curve (1) in the figure is calculated from Eq. (4), and curves (2) and (3) were obtained from Ref. 4. Although it is seen that the magnitude of the Gryzinski cross section is about half that of the experimental

ones, it is considered that it is acceptable. Further comments on Gryzinski's method have been made by Rudge (Ref. 5). In this report, we shall use curve (1).

### B. Electron Impact Ionization of Excited Mercury Atoms

The term diagram of the first few states of mercury is shown in Fig. 2a, where  $6^3P_1$  is the resonance state and  $6^3P_2$  and  $6^3P_0$  are metastable states. If we assume that ionization can take place from all three of these states, we may lump them into a single one and take the ionization potential to be the center of gravity of the three as shown in Fig. 2b. If the Boltzmann relation between the ground state ( $6^1S_0$ ) and the first excited (6P) states is assumed, the 6P-state population density would be populated according to the relation

$$\frac{n(6P)}{n(6^1S_0)} = \frac{g(6P)}{g(6^1S_0)} e^{-5.21/T_e}, \quad (5)$$

where  $T_e$  is the electron temperature in electron volts and  $g$  is the statistical weight of each state.

In writing Eq. (5), it is assumed that the LTE condition holds. However, in an active arc, this condition cannot be satisfied, since bound electron temperatures, particularly in the lower excited states, deviate considerably from those of free electrons. This relation has been investigated in detail for a cesium plasma (Ref. 6).

In an active arc, the population density in the 6P-state is obtained by solving the rate equation

$$\begin{aligned} \frac{dn(6P)}{dt} = & - n(6P)n_e K(6P, C) - n(6P)n_e \sum_{q \neq 6P} K(6P, q) \\ & - n(6P)A(6P, 6^1S_0) - \alpha_m n^2(6P) - D^* \nabla^2 n(6P) \\ & + n_e \sum_{q \neq 6P} n(q)K(q, 6P) + \sum_{q > 6P} n(q)A(q, 6P) \\ & + n_e^2 \left[ n_e K(C, 6P) + \beta(6P) \right], \end{aligned} \quad (6)$$

where  $n(6P)$ ,  $n(q)$ , and  $n_e$  are the densities of the 6P-state, q-state, and free electrons;  $K(6P, q)$  is the collisional transition coefficient from the 6P-state to the q-state;  $K(6P, C)$  is the collisional transition coefficient from the 6P-state to the continuum;  $A(6P, q)$  is the radiative transition probability from the 6P-state to the q-state;  $\beta(6P)$  is the two-body radiative recombination to the 6P-state;  $D^* \nabla^2 n(6P)$  is the diffusion loss term to the wall, and  $\alpha_m$  is the ionization coefficient of the excited-state interactions. (The excited-state interaction ionization will be considered in detail in the next section.) Although the population density of the 6P-state is governed by the rate equation (6), an estimate can be made using the Boltzmann relation. The resonance radiation of the  $6^3P_1$ -state is always trapped (Refs. 6, 7), so that the  $6^3P_1$ -state is always in equilibrium with the ground state at a temperature not too far from the free electron temperature. However, if it is assumed that the 6P state is in equilibrium with the ground state at the free electron temperature, the density of the 6P-state will be overestimated by use of the Boltzmann relation. In the case of cesium, the calculation has been as high as 30% in the temperature range of 2000-4000 K.

The total rate of ionization from the 6P-state can be calculated by

$$\begin{aligned} Z_{2C} &= n_e n(6P) K(6P, C) \\ &= n_e n(6P) \int_{\epsilon_{th}}^{\infty} v(\epsilon) \epsilon^{1/2} f(\epsilon) Q_{2C}(\epsilon) d\epsilon. \end{aligned} \quad (7)$$

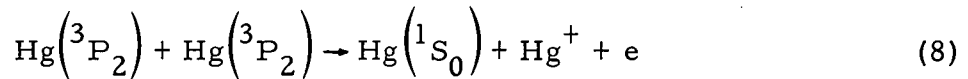
The ionization cross sections of 6P, calculated from Ref. 2, are shown in Fig. 3. Curves (1), (2), and (3) correspond to the  $3P_0$ ,  $3P_1$ , and  $3P_2$  states, respectively. Curve (4) in the figure is the ionization cross section of the lumped state. A simplified model of the rate equation is described below.

It is believed in plasma physics (Ref. 6) that the upper excited states are always nearly in equilibrium with the free electrons. This means that once the bound electron has been excited into the upper states from the 6P-state, it has a good chance of being ionized. In other words, the ionization results mainly from the lower energy states, particularly the first excited state (in mercury, the 6P-state). In this treatment, we assume that

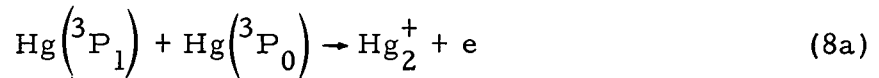
the levels beyond the  $6P$ -state are in equilibrium with the continuum; and hence the population density can be calculated by the Saha equation from the known electron density and electron temperature. In this case, the rate equation can be readily solved algebraically if we use the bulk plasma limit (i. e., volume  $V \rightarrow \infty$ , total number of particles  $N \rightarrow \infty$ , and  $n = N/V < \infty$ ) and the steady-state condition.

### C. Ionization Due to Excited-State Atom Collisions

It is possible for the atoms in the metastable or resonance states of mercury to collide with each other and produce ionization. These processes may be due to



for atomic ions and



for molecular ions. The last step is a collision between atoms in a metastable and a resonance state. The collision cross section given by von Engel (Ref. 8) is of the order of  $10^{-13} \text{ cm}^2$ . Although it is expected that process (8a) occurs in preference to process (8) because the ionization potential of molecular mercury is lower than that of atomic mercury, process (8) is considered equally important in producing ionization. Processes analogous to (8) and (8a) have been studied for inert gas discharges in connection with the mechanism of ionization (Refs. 9, 10).

The ionization cross sections for the excited-state interactions are not available. However, estimates have been made for inert gases (Refs. 9, 11). For helium, the ionization cross section of the interaction of two metastable states has been estimated to be of the order of  $10^{-14}$  (Ref. 11); and, as mentioned above, the cross section of process (8a) as given by von Engel is of the order of  $10^{-13} \text{ cm}^2$ . These values indicate that the ionization cross section for processes (8) and (8a) is of the order

of  $10^{-14} \text{ cm}^2$ . Taking this value for the ionization cross section, the ionization coefficient of processes (8) and (8a) can be calculated readily as

$$\alpha_{\text{mm}} = Q(6\text{P}, 6\text{P}) \bar{v}_m, \quad (9)$$

where  $\bar{v}_m$  is the mean velocity of the 6P-state atoms. The rate of ionization then is

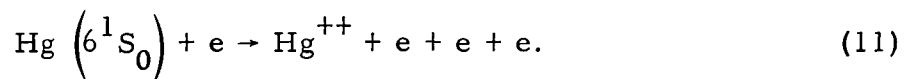
$$Z_{\text{mm}} = \alpha_{\text{mm}} n^2(6\text{P}). \quad (10)$$

### III. DOUBLE IONIZATION PROCESSES

Doubly ionized particles that have been detected in the thruster beam analysis may be the result of (1) direct neutral ground-state ionization by energetic electron impact, and (2) ionization of ions due to electron impact (Ref. 12).

#### A. Direct Neutral Ground-State Ionization by Electron Impact

Although the double ionization potential for mercury is quite high (29.4 eV from  $6^1\text{S}_0$ ), it is still possible to produce ionization by electron bombardment. This process may be of the type



Gryzinski (Ref. 2) has also developed a method for calculating the multiple ionization cross section due to electron impact, which is expressed by the equations

$$\begin{aligned} e^{Q_{\text{sc}}^{++}} &= \frac{2}{4\pi r^2} \left(\frac{\sigma_0}{V_i^2}\right) \left(\frac{\sigma_0}{V_{ii}^2}\right) \\ &\times \left[ g_Q(V, \epsilon; V_i) - \left(\frac{V_i}{\epsilon - V_{ii}}\right) g_Q(V, \epsilon; \epsilon - V_{ii}) \right] \\ &\times g_Q(V, \epsilon - \langle \Delta E_{\text{sc}} \rangle; V_{ii}) \end{aligned} \quad (12)$$

$$\begin{aligned}
e^{Q_{ej}^{++}} &= \frac{2}{4n\bar{r}^2} \left( \frac{\sigma_0}{V_i^2} \right) \left( \frac{\sigma_0}{V_{ii}^2} \right) \\
&\times \left[ \left( \frac{V_{ii}}{V_i + V_{ii}} \right)^2 g_Q(V, \epsilon; V_i + V_{ii}) \right. \\
&\left. \times g_Q(V, \langle \Delta E_{ej} \rangle; V_{ii}) \right] \tag{13}
\end{aligned}$$

$$e^{Q_{total}^{++}} = e^{Q_{sc}^{++}} + e^{Q_{ej}^{++}} \tag{14}$$

where  $\sigma_0$  is equal to  $6.56 \times 10^{-14} \text{ cm}^2 - eV^2$ ,  $\bar{r}$  is the mean distance between two interacting electrons,  $V_i$  is the ionization energy of first electron,  $V_{ii}$  is the ionization energy of second electron,  $g_Q$  is the functional dependence of the cross section on the incident electron energy,  $\epsilon$  is the incident electron energy, and  $V$  is the binding energy of the bound electron. The terms  $\langle E_{sc} \rangle$  and  $\langle \Delta E_{ej} \rangle$  are expressed as

$$\langle \Delta E_{sc} \rangle \cong \frac{\ln \left[ \frac{(\epsilon - V_{ii})}{V_{ii}} \right]}{1 - \frac{V_i}{\epsilon - V_{ii}}} \tag{15}$$

$$\langle \Delta E_{ej} \rangle \cong (V_i + V_{ii}) \frac{\ln \left[ \frac{\epsilon}{V_i + V_{ii}} \right]}{1 - \frac{V_i + V_{ii}}{\epsilon}} \tag{16}$$

$$\begin{aligned}
g_Q(\epsilon, V; V_i) &= \left( \frac{V}{\epsilon} \right) \left( \frac{\epsilon}{\epsilon + V} \right)^{3/2} \\
&\times \left\{ \frac{V_i}{V} + \frac{2}{3} \left( 1 - \frac{V_i}{2\epsilon} \right) \ln \left[ 2.7 + \left( \frac{\epsilon - V_i}{V} \right)^{1/2} \right] \right\} \\
&\times \left( 1 - \frac{V_i}{\epsilon} \right)^{1 + \frac{V}{V + V_i}}, \tag{17}
\end{aligned}$$

Gryzinski also gave an estimate of the mean distance  $\bar{r}$  by matching to the value of the experimental cross section. This estimate can be expressed as

$$\bar{r} \cong \frac{\sigma_0}{V_i V_{ii}} \left( \frac{2}{4\pi} \frac{0.058}{Q_{\max}^{++}} \right)^{1/2}, \quad (18)$$

where  $Q_{\max}^{++}$  is the maximum value of the cross section for mercury as given by Bleakney (Ref. 4):

$$Q_{\max}^{++} = 7 \times 10^{17} \text{ cm}^2, \quad (19)$$

resulting in a value of

$$\bar{r} = 0.38 \text{ \AA}. \quad (20)$$

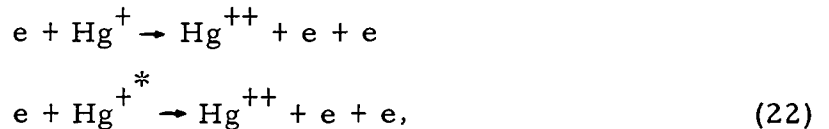
The double ionization cross section thus calculated is shown in Fig. 4.

Having obtained the cross section, the rate of double ionization due to direct electron impact can be calculated as

$$Z^+ = n_e n \left( {}^1S_0 \right) \int_{\epsilon_{\text{th}}}^{\infty} v(\epsilon) \epsilon^{1/2} f(\epsilon) e Q^{++}(\epsilon) d\epsilon. \quad (21)$$

#### B. Ionization From a Singly Ionized Ion

Another means of producing double ionization is by electron impact on singly ionized ions. The processes are



where  $\text{Hg}^{+*}$  is the excited ion and can be produced by (Ref. 13)



The cross sections of (22) and (23) as a function of electron energy are unknown. Again, an estimate using available information on the double-to-single ion current ratio (Ref. 12) must be made. Massey (Ref. 13) has given the expression for the ionization cross section for an ion as

$$Q_i^+ = \frac{i_{++}}{i_+ i_e} \frac{he v_e V_+}{2(v^2 + V_+^2)^{1/2}} F \quad (24)$$

and

$$F = \frac{\int_0^h i_+(z) dz \int_0^h i_e(z) dz}{h \int_0^h i_+(z) i_e(z) dz}, \quad (25)$$

where  $i_+$ ,  $i_{++}$ , and  $i_e$  are the currents of the single ion, double ion, and electron beam;  $h$  is the height of the ion beam,  $v_e$  is the electron velocity, and  $V_+$  is the ion velocity. If we take  $F$  to be unity and  $v_e \gg V_+$ , then Eq. (24) takes the form

$$Q_i^+ = \frac{i_{++}}{i_+ i_e} \frac{eV_+ h}{2}. \quad (26)$$

Substituting the measured ratio  $i_{++}/i_+ = 0.12$  from Ref. 14, and taking  $i_e = i = 500$  mA,  $V_+ = 3 \times 10^4$  cm/s, and  $h = 0.2$  cm, we obtain

$$Q_i^+ = 2.2 \times 10^{-16} \text{ cm}^2 \quad (27)$$

This is in good agreement with the earlier measured value of  $4.2 \times 10^{-6} \text{ cm}^2$  (Ref. 15). Here we have taken the mean ion velocity to be  $3 \times 10^4$  cm/s, which corresponds to an ion temperature  $T_+ = 1000$  K. The effective ionization coefficient of ions by electron impact is then

$$\alpha_i^+ = Q_i^+ v_e, \quad (28)$$

and the total production rate of doubly ionized ions can be calculated as

$$Z_i^+ = n_e^2 \alpha_i^+ = n_e^2 Q_i^+ \bar{v}_e. \quad (29)$$

#### IV. RESULTS AND DISCUSSION

We have discussed various collisional ionization processes in mercury discharges. Collisional cross sections are taken mostly from calculations using Gryzinski's classical approximation. The collisional ionization coefficients of the various states are derived by integrating the product of the cross section and electron energy distribution function over the whole energy space. It should be mentioned that the calculations presented here have also been made using the analytical approximation given by Goldstein (Ref. 3):

$$K(p, q) = \frac{1}{V_{pq}^{3/2}} \frac{3.84 \times 10^{-6} y^t e^{-y}}{A^{1/4} \left( y^2 + \frac{7y}{4} + \frac{1}{9} \right)}, \quad (30)$$

where  $y = V_{pq} / T_e$  and  $A = V_p^i / V_{pq}$ , with  $V_{pq}$  being the energy needed for the transition from the p-state to q-state (in eV),  $V_p^i$  the binding energy of the p-th state (in eV), and

$$t = \frac{A + 30}{5(2A + 5)}. \quad (31)$$

Figure 5 illustrates the collisional ionization coefficients by direct electron impact. This calculation has also been made by Masek (Ref. 14). The figure also shows the double ionization coefficient. It can be seen that the ratio of the double- to the single-ionization rate ranges from  $10^{-6}$  at low electron temperatures to about  $10^{-2}$  at high electron temperatures. It is therefore concluded that direct electron impact is less likely to produce double ionization, and that electron-ion impact collisions are probably mostly responsible for producing doubly ionized ions.

The collisional ionization coefficients from 6P-states by electron impact are shown in Fig. 6, with solid lines representing the 6P-states and open circles the lumped (6P) state.

It may be worthwhile here to show the calculated excited-state mercury density by solving the rate equation (6) using a simplified model, as discussed in Section II-B. Presuming a bulk plasma limit, we make the assumption that the resonance radiation is completely trapped; i. e.,  $g = 0$ , where  $g$  is the escape factor of the resonance radiation. The 6P-state population density thus calculated as a function of electron density is shown in Fig. 7a, with electron temperature as a parameter. It is seen that for a specific electron temperature the true excited-state density is close to the Boltzmann density only when the electron density is high. Therefore, high electron density not only makes the distribution function Maxwellian, it also ensures that the bound electrons will be Boltzmann and hence guarantees an LTE condition of the plasma. However, in the low electron density limit, the deviation from the Boltzmann relation is considerable because there is a lack of the electron-electron interaction needed to ensure an LTE condition. Irregularities at  $T_e = 0.5$  eV and  $n_e = 10^{15}$  cm<sup>-3</sup> are due to high electron density and low electron temperature, which are the extreme limits of the cases considered. Figure 7b is a counterplot of Fig. 7a, with electron density (ionization fraction  $\alpha$ ) as a parameter. Both Figs. 7a and 7b are fixed at a neutral density  $n_a = 10^{16}$  cm<sup>-3</sup>.

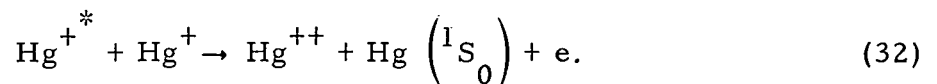
Figures 8a through 8d show the ion production rates as a function of electron temperature at a neutral atom density  $n_a = 10^{16}$  cm<sup>-3</sup>, with the degree of ionization varying from  $10^{-1}$  to  $10^{-5}$ . For all these escape probabilities  $g = 0$ . It is seen immediately that the two-step ionization dominates over the other processes at intermediate and high electron temperatures ( $T_e \geq 1$  eV) except when the degree of ionization is very low (i. e., for  $\alpha \leq 0.01$ ). On the other hand, the ionization due to excited 6P-state interactions is more significant than the other processes when the degree of ionization is low ( $\alpha \leq 10^{-3}$ ). It is easily seen that at a higher degree of ionization the electron is important in all kinds of collision processes, including ionization, since the electrons collide with heavy particles as well as electrons themselves more frequently. Higher collision frequency between electrons and atoms produces higher ionization and excitation rates, and higher interelectron interaction ensures that the electron will be Maxwellian. In the limit of a low degree of ionization, the electron collision rate is not sufficient to produce appreciable ionization, and heavy particle collisions then dominate.

It is also interesting to note that, although the direct process cannot be a decisive factor in producing ionization, it is a competitive mechanism for a low degree of ionization at high temperatures. This can be seen from Figs. 8c and 8d. Figure 8d shows that the direct ionization is one order of magnitude higher than the two-step ionization, because there is not sufficient density for the ionization in the excited state when the degree of ionization is low.

Temperature effects on the ion production rates are significant. However, the functional form of the rate dependence on the temperature is essentially the same as that of the collisional transition coefficients. At lower electron temperature limits, we see that both  $Z_{1c}$  and  $Z_{2c}$  drop faster than  $Z_{mm}$ . This is the case because both  $K_{1c}$  and  $K_{2c}$  drop fast at low electron temperatures, while  $K_{mm}$  is essentially constant, depending on atom temperature only.

It should be noted here that, although the above conclusions are drawn only for the single neutral density at  $n_a = 10^{16} \text{ cm}^{-3}$ , the relative magnitudes of  $Z_{1c}$ ,  $Z_{2c}$ , and  $Z_{mm}$  remain the same over other neutral densities for the same degree of ionization.

Figure 9 presents the double ion production rates for single-step and two-step (from singly ionized ions) processes. It is seen that the ionization from ions is more important than that from neutrals. This is due to the fact that ionization from ions (or excited ions) has a larger ionization cross section and lower ionization potential than that of the neutral ground state. The double ionizations, other than the two mentioned in this study, are considered to be unimportant. There may be processes such as



However, there is not enough information available to support consideration of this process.

In drawing the above conclusions, we have assumed that (1) electrons are Maxwellian at  $T_e$  (where  $T_e$  is the free electron temperature), and (2) the excited 6P-state is calculated from the rate equation, assuming a specific value for the escape factor  $g$ . Assumption (1) can be justified at high

electron density ( $n_e \geq 10^{13} \text{ cm}^{-3}$ ), where the electron-electron Coulomb interaction is very effective in making the electron energy transfer Maxwellian. However, when the degree of ionization is low, the electron collides primarily with neutral atoms, so that a Maxwellian electron may not be obtainable. In that case, the distribution function  $f(\epsilon)$  in the integration in Eqs. (2), (3), (7), and (21) should be replaced by a true distribution function. Electric field effects on the ion production rate can be examined through the calculation of electron distribution function in the electric field by the kinetic theory.

The non-Maxwellian effects on the ionization have been investigated in Ref. 10. In general, first, the non-Maxwellian electron reduces the collisional transition (ionization and excitation) coefficients because of the depletion of the electron distribution function in the high-energy part due to inelastic collision. Secondly, the non-Maxwellian distribution also affects the  $n(6P)$  density calculation because of changes in transition coefficients. These points will be left for further investigation.

It is noted here that a group of high monoenergetic electrons has been detected (Ref. 16) in ion thrusters. This group of electrons, known as the "primary electrons," has an energy up to about 30 eV. The portion of primary electrons (given in Ref. 16) can be up to 10% of the total electron density. Assuming that this group of electrons is distributed by a delta function, the ion production rate can be integrated readily and expressed as

$$Z_{1c}^P = n_p n \left( {}^1S_0 \right) Q_{1c}(\epsilon_p) v_p, \quad (33)$$

where  $n_p$ ,  $\epsilon_p$ , and  $v_p$  are the primary electron density, energy, and velocity, respectively.

The rate coefficients decay slowly and are relatively constant at higher electron temperatures. Because  $Q \propto \ln E/E$  and  $v \propto E^{1/2}$ ,  $Z_{1c}^P \propto \ln E/E^{1/2}$  is a relatively constant value over the high electron temperature of interest. The evaluation of  $Z_{1c}$  then strongly depends on the primary electron density. An estimate of the ionization rate due to the primary electrons indicates that  $Z_{1c}^P$  is of the same order as  $Z_{1c}$ , the direct ionization rate by thermal electrons. The ionization due to primary and thermal electrons is about equal

when the ratio  $n_p/n_e$  is high ( $\gamma = n_p/n_e > 0.01$ ). In this case, the primary electrons will play an important role in the ionization within ion thrusters.

In dealing with the rate equation (6), we have assumed a bulk plasma model in which we neglect the diffusion loss and take the resonance radiation to be completely imprisoned. However, in an actual discharge case, this cannot be true, and the g-value should come from solving the radiative transfer equation by specifying a discharge geometry (a cylinder in a hollow cathode). Figure 10 shows how different values of the escape factor g will affect the excited-state density. It can be seen that the excited-state population is lower for a higher degree of escape probability. Evidently, the g-value is the controlling factor for excited-state density.

## REFERENCES

1. Goldstein, R., Pawlik, E. V., and Wen, Liang-Chi, Preliminary Investigations of Ion Thruster Cathodes, Technical Report 32-1536, Jet Propulsion Laboratory, Pasadena, Calif., Aug 1, 1971.
2. Gryzinski, M., "Classical Theory of Atomic Collision, I. Theory of Inelastic Collisions," Phys. Rev., Vol. 138, A336, 1965.
3. Goldstein, R., Numerical Calculation of Electron-Atom Excitation and Ionization Rates Using Gryzinski Cross Sections, Technical Report 32-1372, Jet Propulsion Laboratory, Pasadena, Calif., Mar. 1, 1969.
4. Kieffer, L. J., "Low-Energy Electron-Collision Cross Section Data," Atomic Data, Vol. 1, pp. 19-97, 1969; Vol. 1, pp. 121-287, 1969; Vol. 2, pp. 293-391, 1971.
5. Rudge, M. R. H., "Theory of the Ionization of Atoms by Electron Impact," Rev. Mod. Phys., Vol. 40, p. 564, 1968.
6. Norcross, D. W., and Stone, P. M., "Recombination, Radiative Energy Loss and Level Population in Nonequilibrium Cesium Discharges," JQSRT, Vol. 8, p. 655, 1968.
7. Holstein, T., "Imprisonment of Resonance Radiation in Gases," Phys. Rev., Vol. 72, p. 1212, 1947; Vol. 83, p. 1159, 1951.
8. von Engle, A., Ionized Gases, Oxford University Press, Oxford, 1965, p. 76.
9. Salinger, S. N., and Rowe, J. E., "Determination of the Predominant Ionization and Loss Mechanisms for the Low-Voltage Arc Mode in a Neon Plasma Diode," J. Appl. Phys., Vol. 39, p. 4299, 1968.
10. Shaw, D. T., "On the Ionization Mechanism for Low-Voltage Neon Plasma Arcs," Energy Conv. Vol. 12, p. 9, 1972.
11. Phelps, A. V., and Molnar, J. P., "Lifetimes of Metastable States of Noble Gases," Phys. Rev., Vol. 89, p. 1202, 1953.
12. Pawlik, E. V., et al., "Ion Thruster Performance Calibration," AIAA Paper 72-475, AIAA 9th Electric Propulsion Conference, Bethesda, Md., April 17-19, 1972.
13. Massey, H. S. W., Electronic and Ionic Impact Phenomena, Vol. I, Clarendon Press, Oxford, Second Ed., 1969.
14. Masek, T. D., Plasma Characteristics of the Electron Bombardment Ion Engine, Technical Report 32-1271, Jet Propulsion Laboratory, Pasadena, Calif., Apr. 15, 1968.

REFERENCES (contd)

15. Latypov, Z. Z., Kupriyanov, S. E., and Tunitskii, N. N., "Ionizing Collisions of Electrons with Ions and Atoms," Sov. Phys-JETP, Vol. 19, p. 570, 1964.
16. Masek, T. D., Plasma Properties and Performance of Mercury Ion Thrusters, Technical Report 32-1483, Jet Propulsion Laboratory, Pasadena, Calif., June 15, 1970.

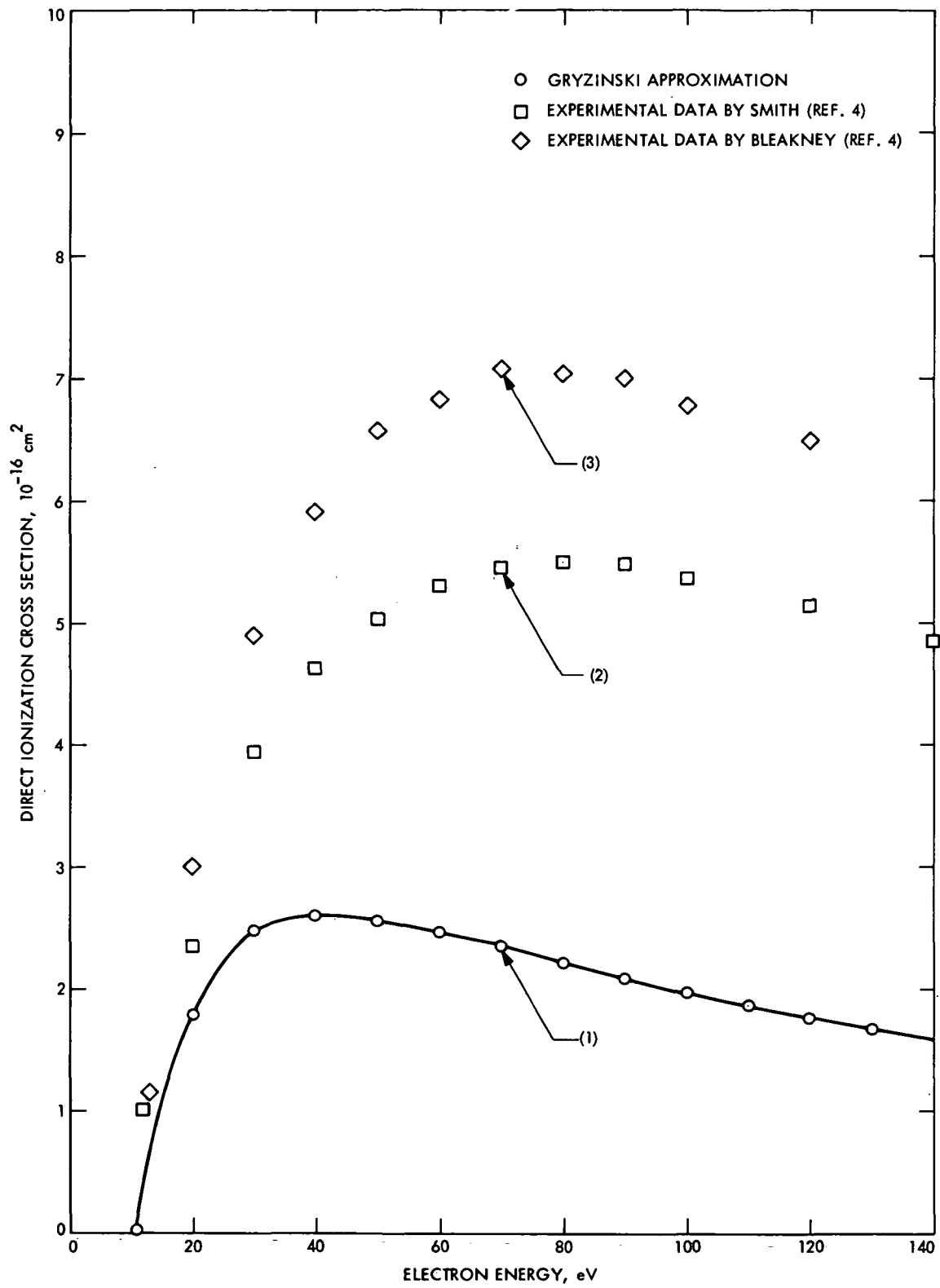


Fig. 1. Direct electron ionization cross sections

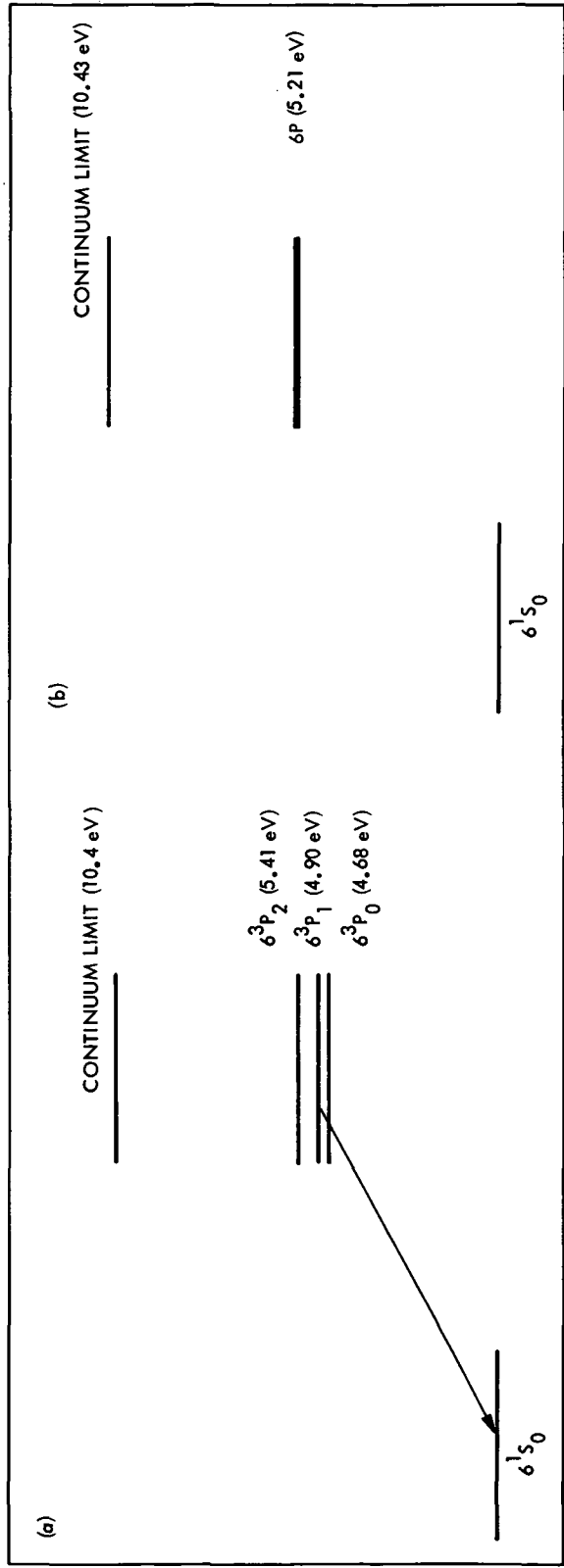


Fig. 2. Energy diagram of the mercury atom

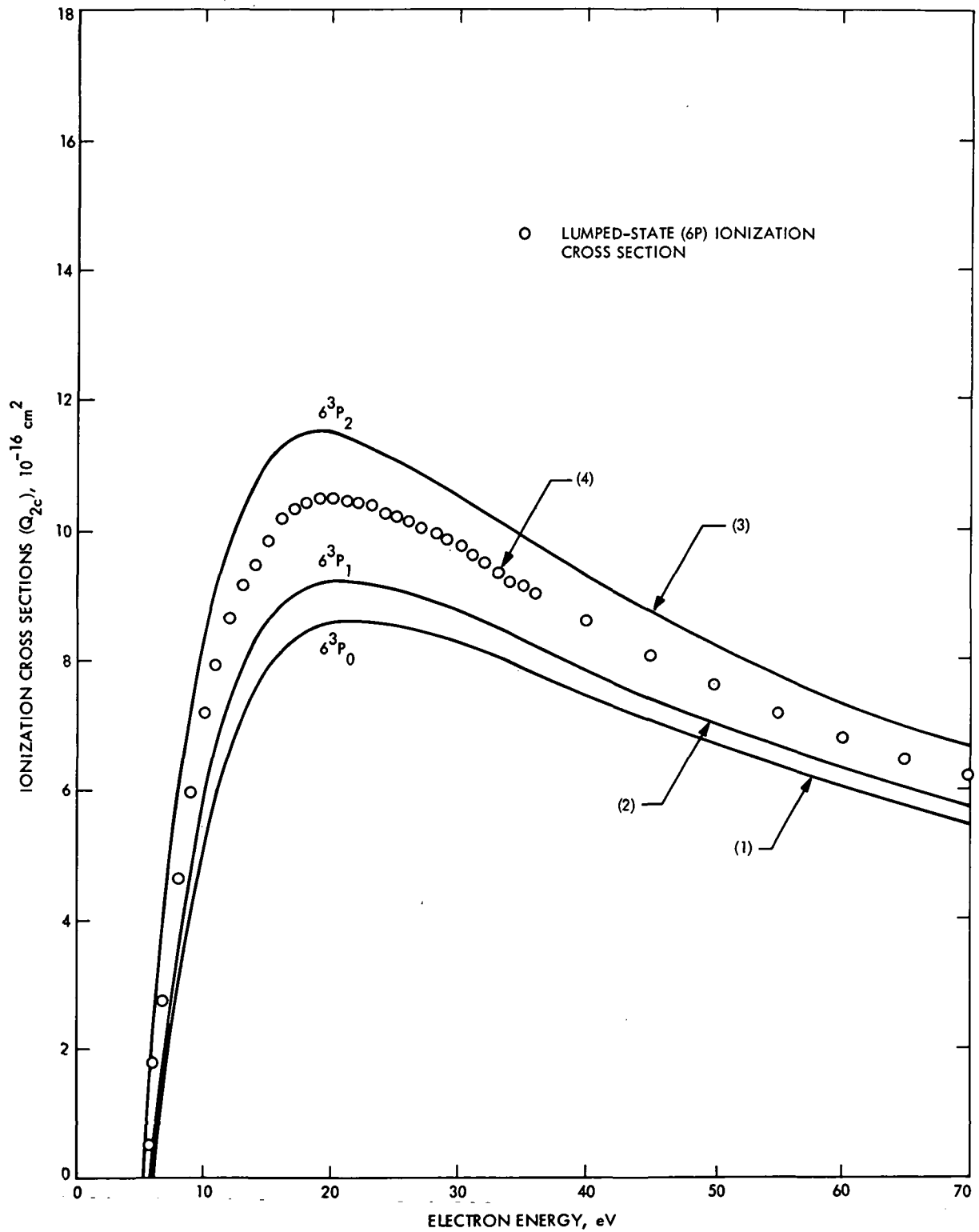


Fig. 3. Ionization cross sections for the 6P-state by electron impact

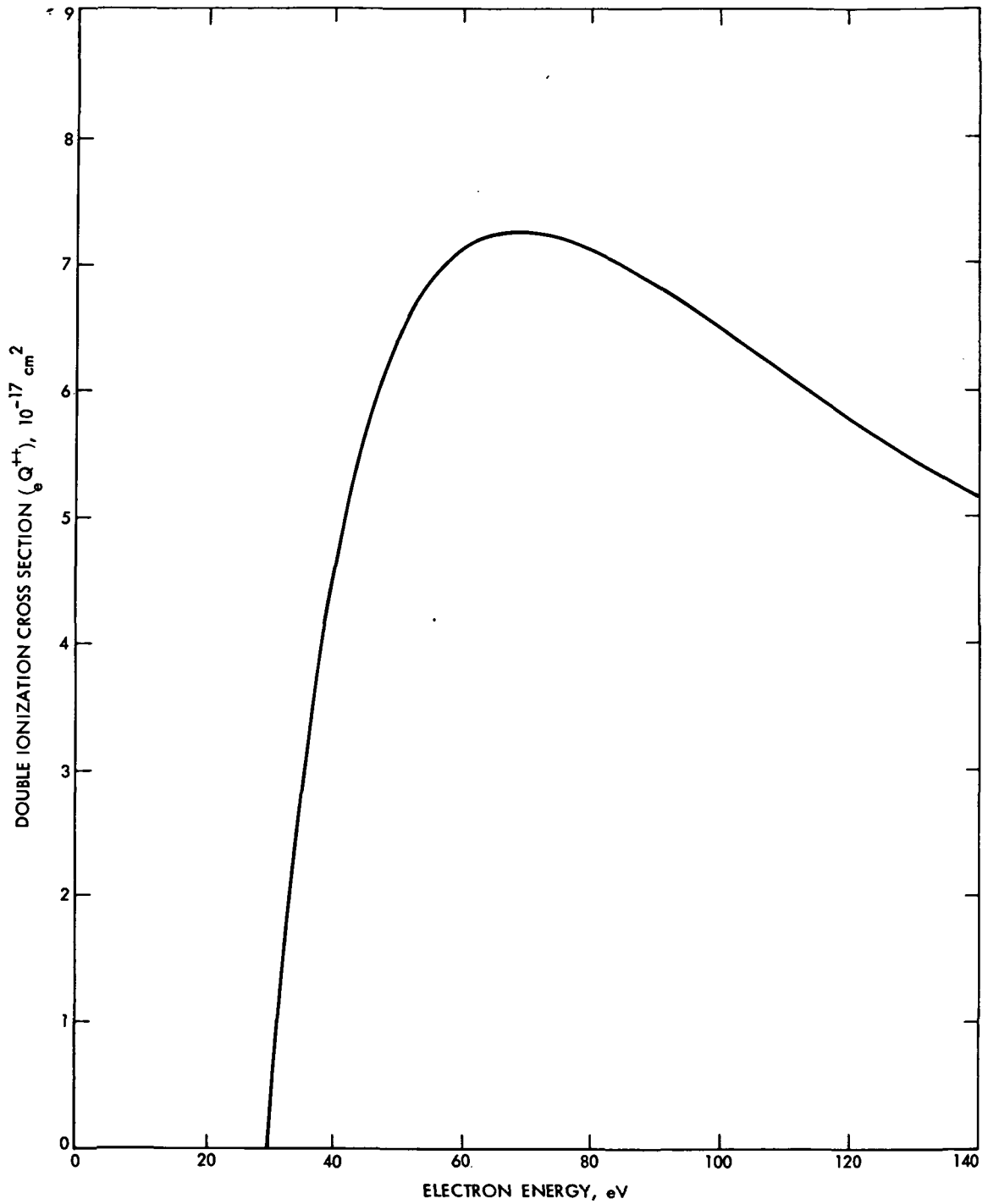


Fig. 4. Direct double ionization cross sections by electron impact

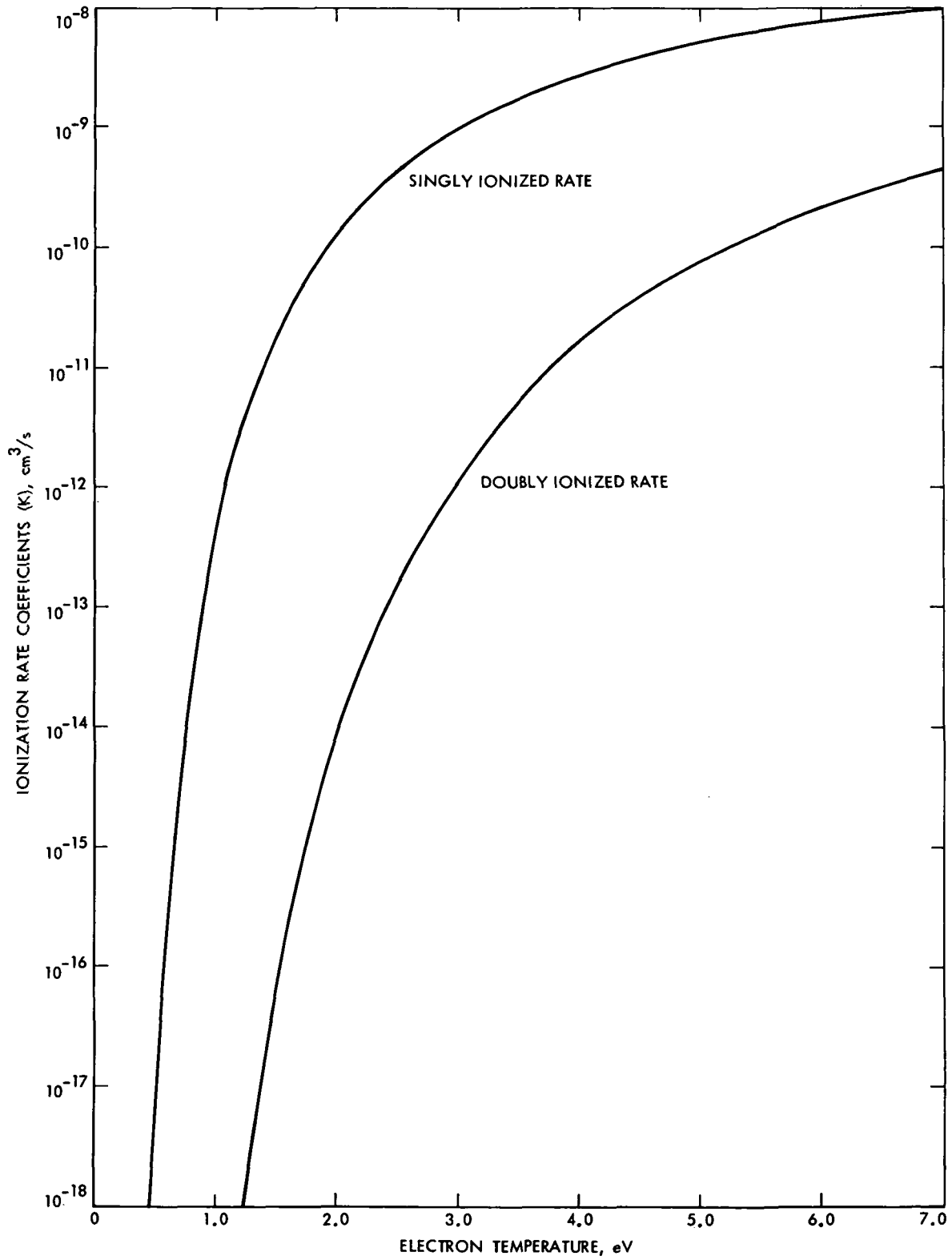


Fig. 5. Singly and doubly collisional ionization coefficients

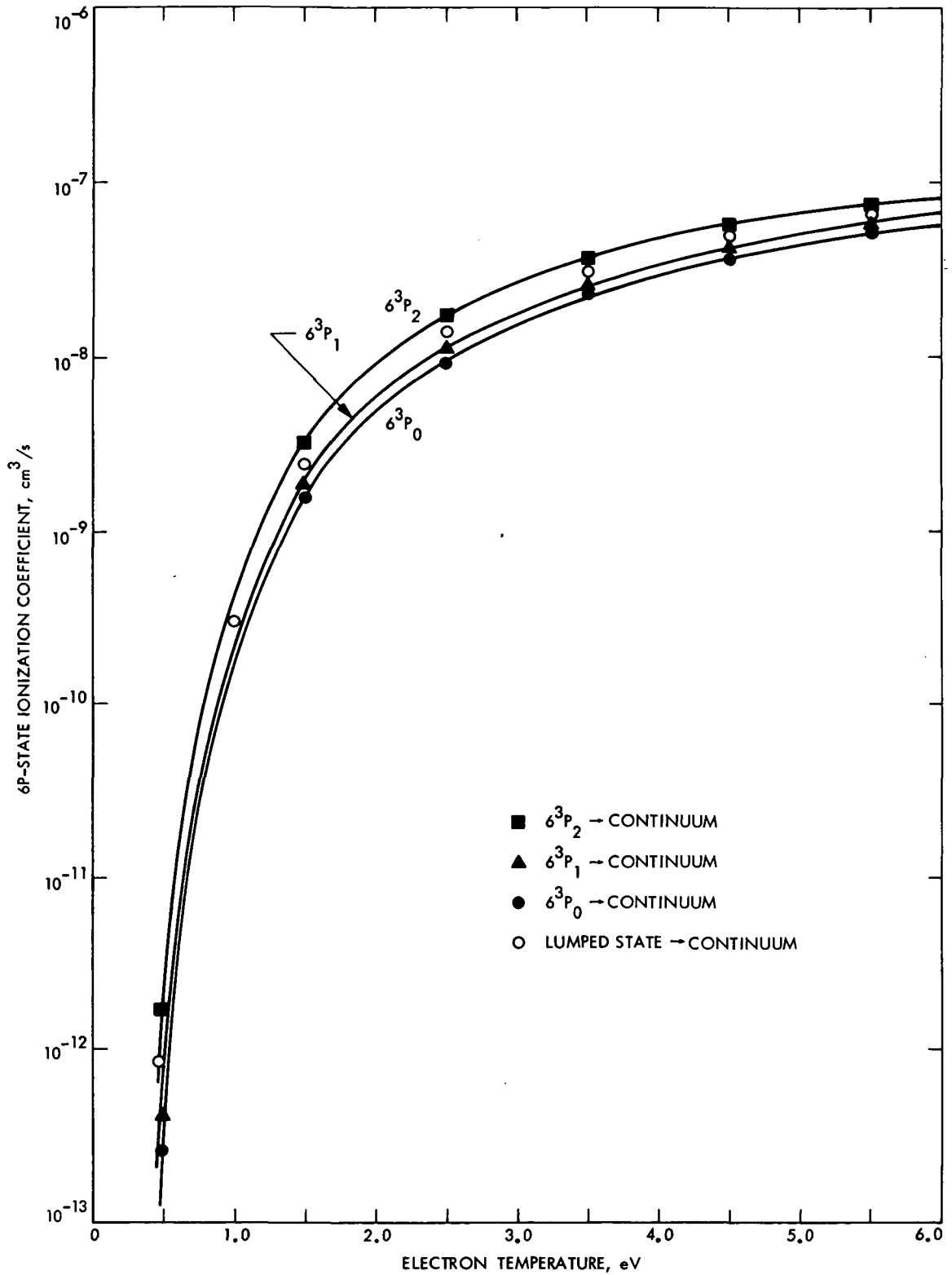


Fig. 6. Collisional ionization coefficients of the 6P-state by electron impact

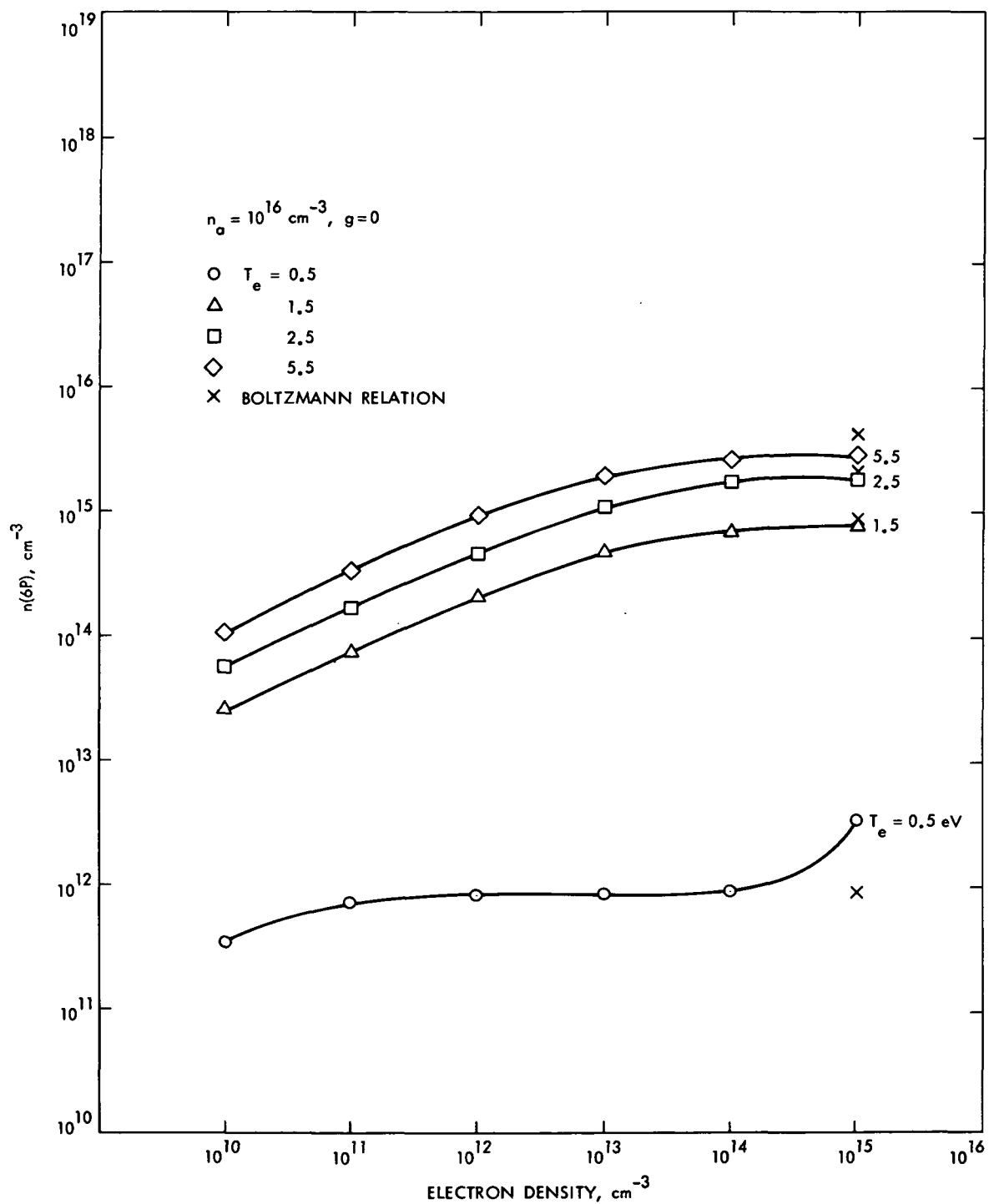


Fig. 7a. Population density  $n(6P)$  vs  $n_e$  for  $T_e = 0.5, 1.5, 2.5,$  and  $5.5 \text{ eV}$  at  $n_a = 10^{16} \text{ cm}^{-3}, g = 0$

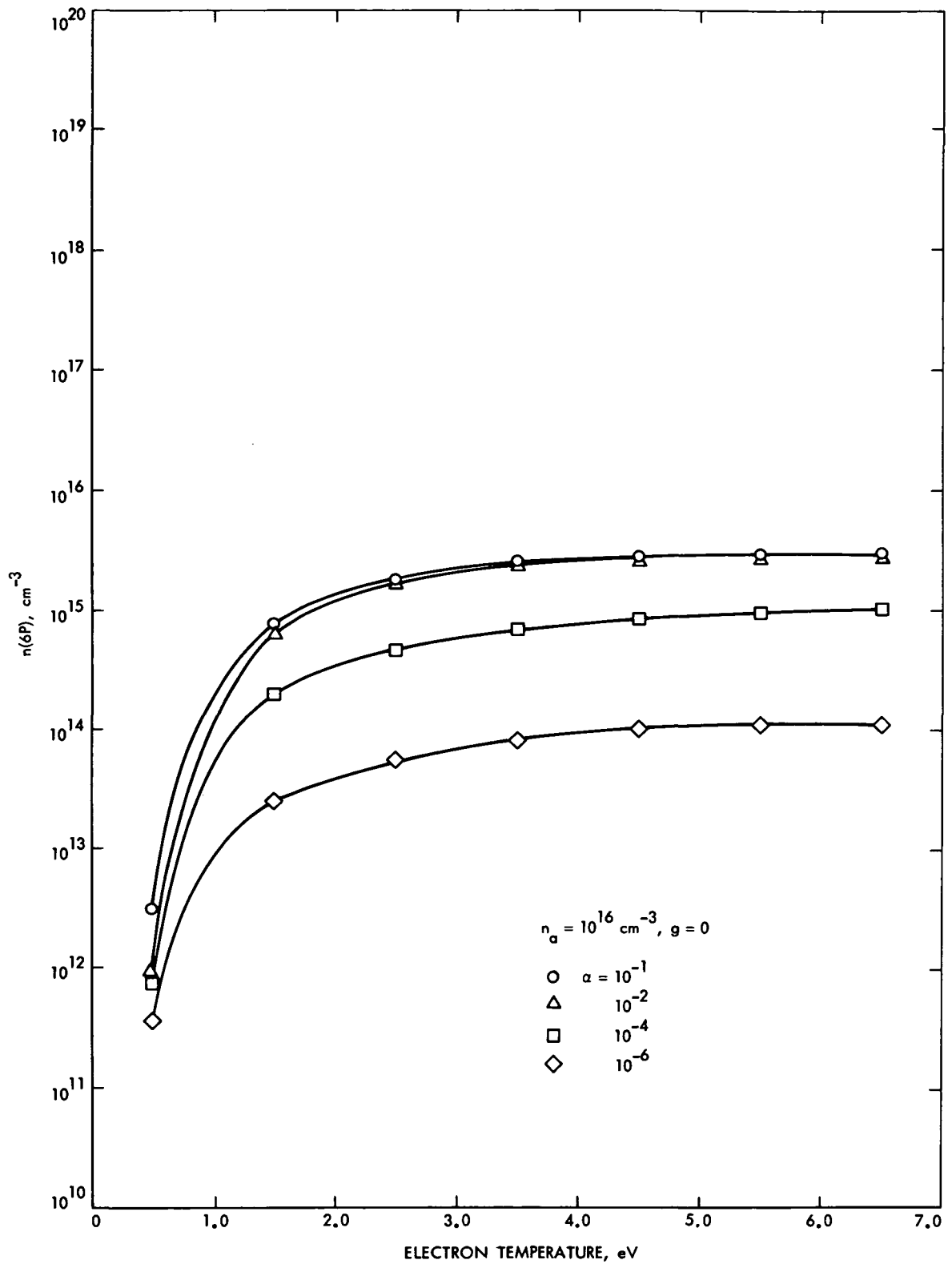


Fig. 7b. Population density  $n(6P)$  vs  $T_e$  for different degrees of ionization at  $n_a = 10^{16} \text{cm}^{-3}$ ,  $g = 0$

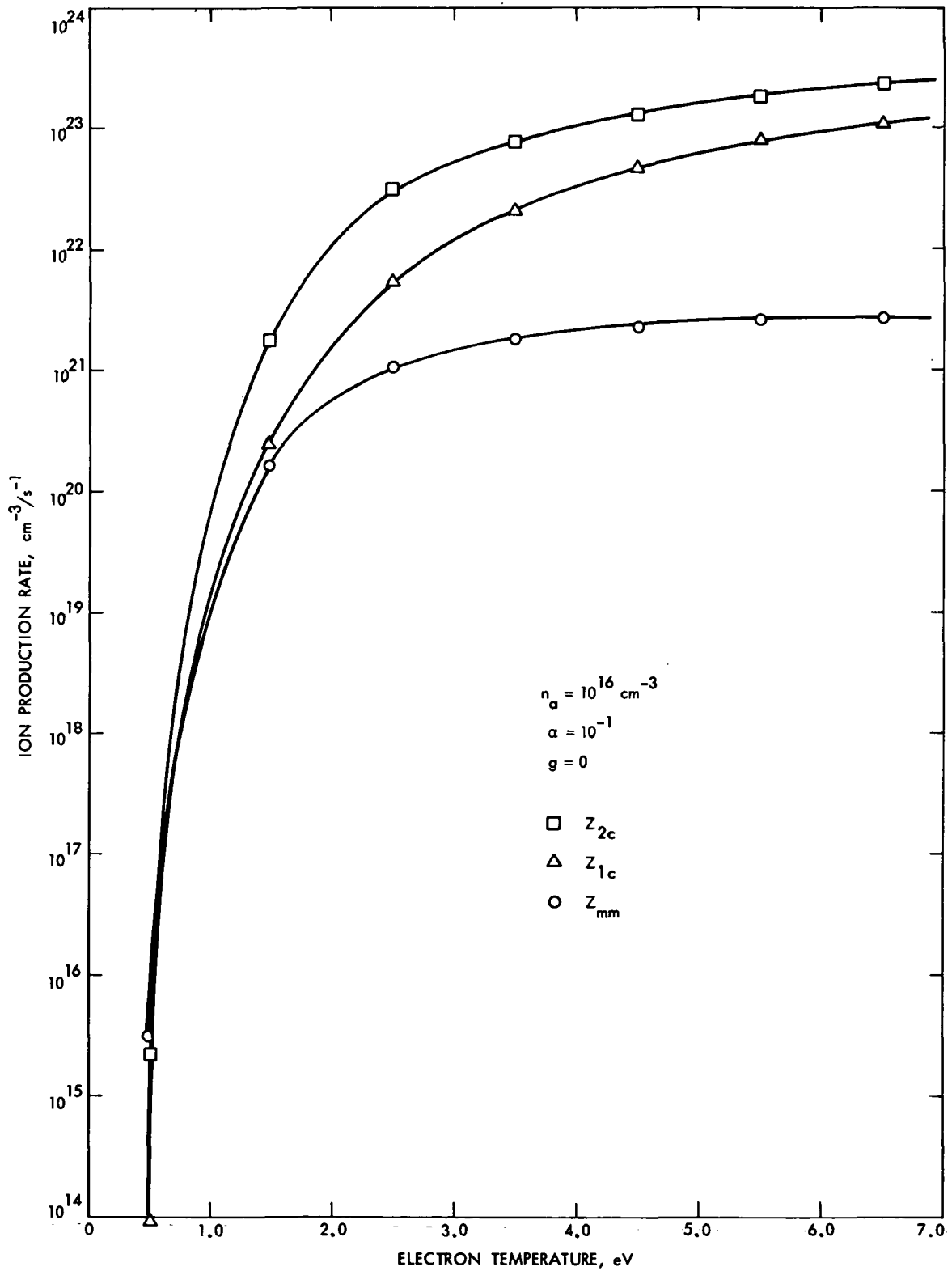


Fig. 8a. Ion production rate at  $n_a = 10^{16} \text{ cm}^{-3}$ ,  $\alpha = 10^{-1}$

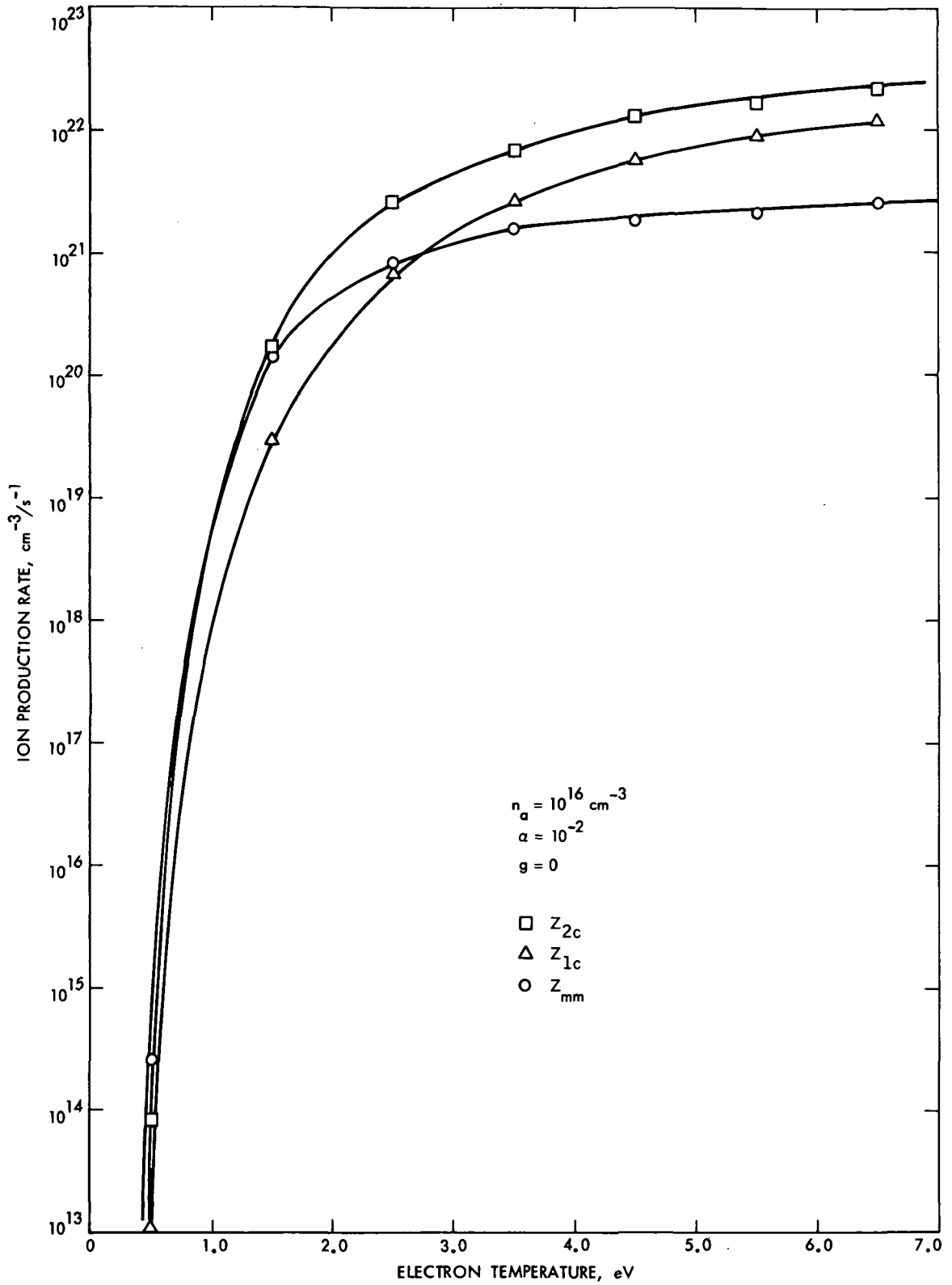


Fig. 8b. Ion production rate at  $n_a = 10^{16} \text{ cm}^{-3}$ ,  $\alpha = 10^{-2}$

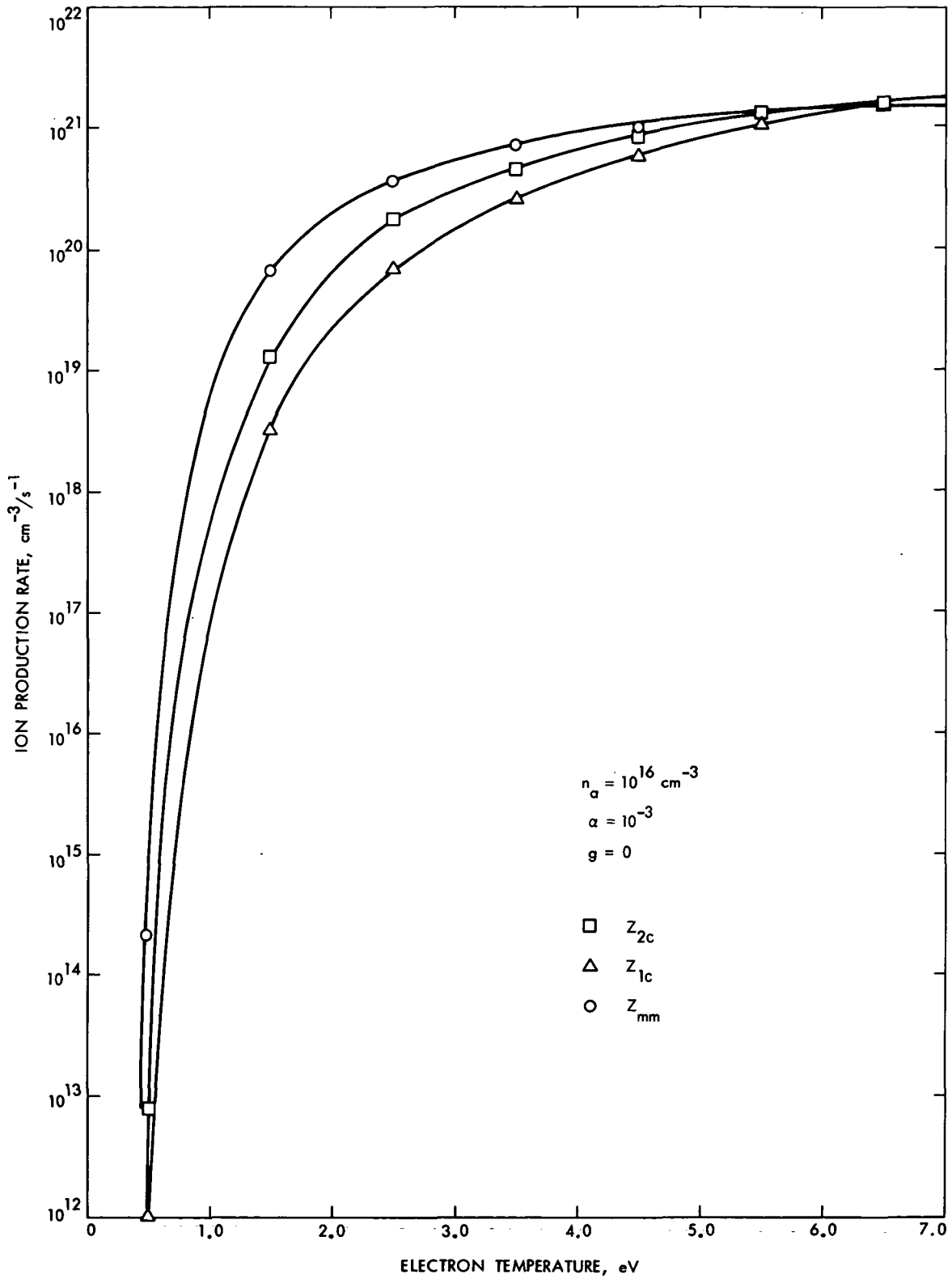


Fig. 8c. Ion production rate at  $n_a = 10^{16} \text{ cm}^{-3}$ ,  $\alpha = 10^{-3}$

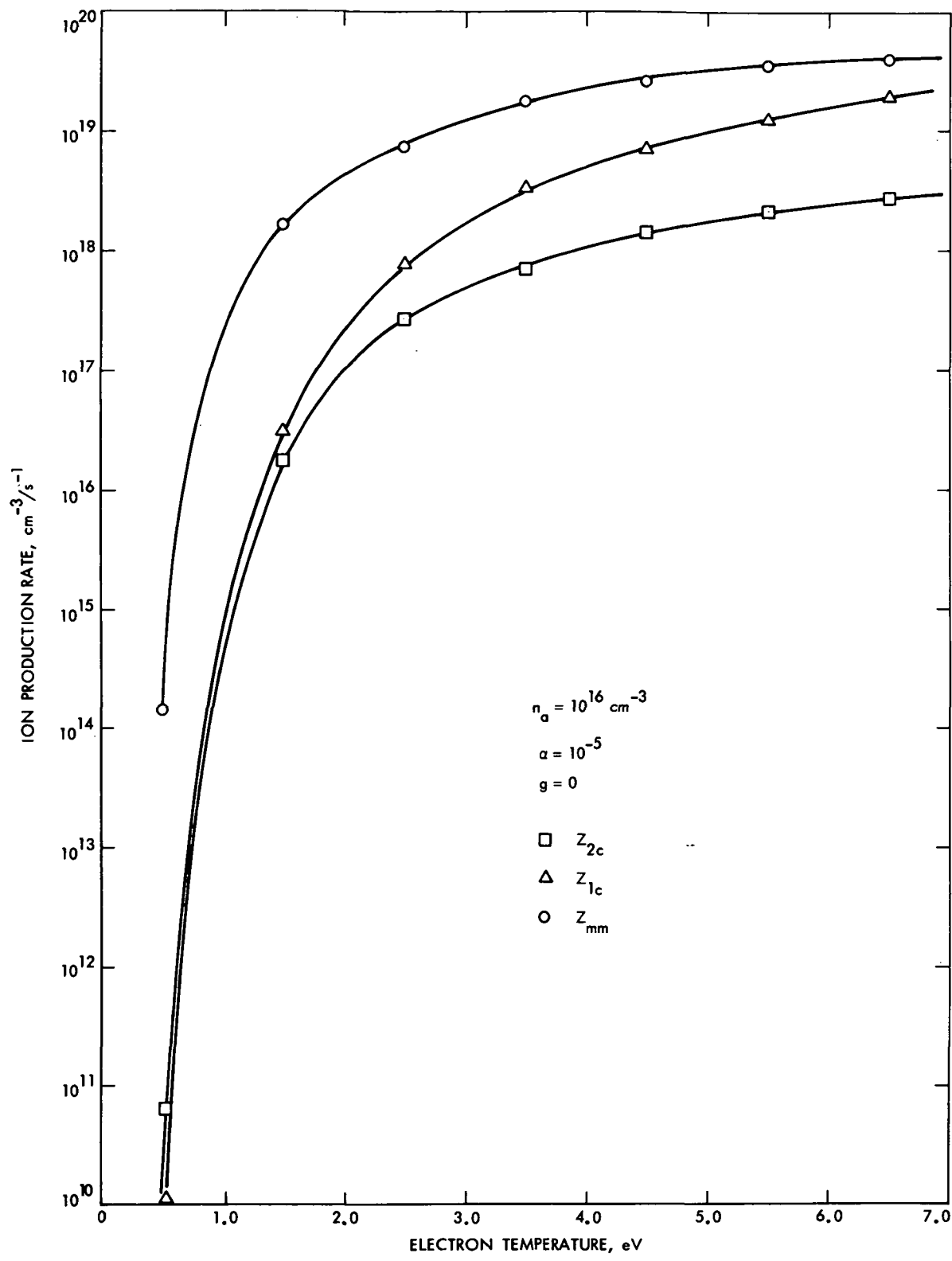


Fig. 8d. Ion production rate at  $n_a = 10^{16} \text{ cm}^{-3}$ ,  $\alpha = 10^{-5}$

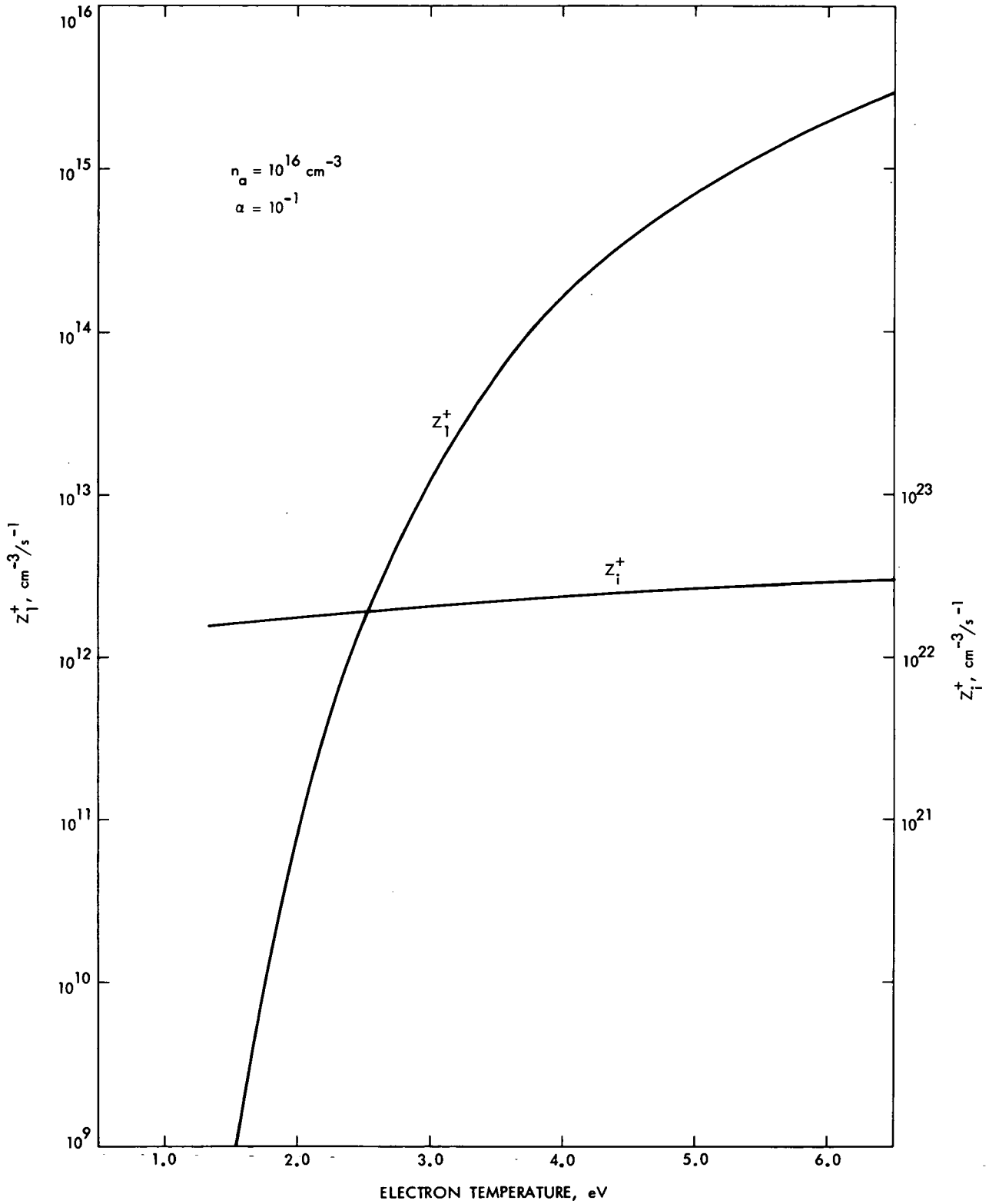


Fig. 9. Double ion production rate at  $n_a = 10^{16} \text{ cm}^{-3}$ ,  $\alpha = 10^{-1}$

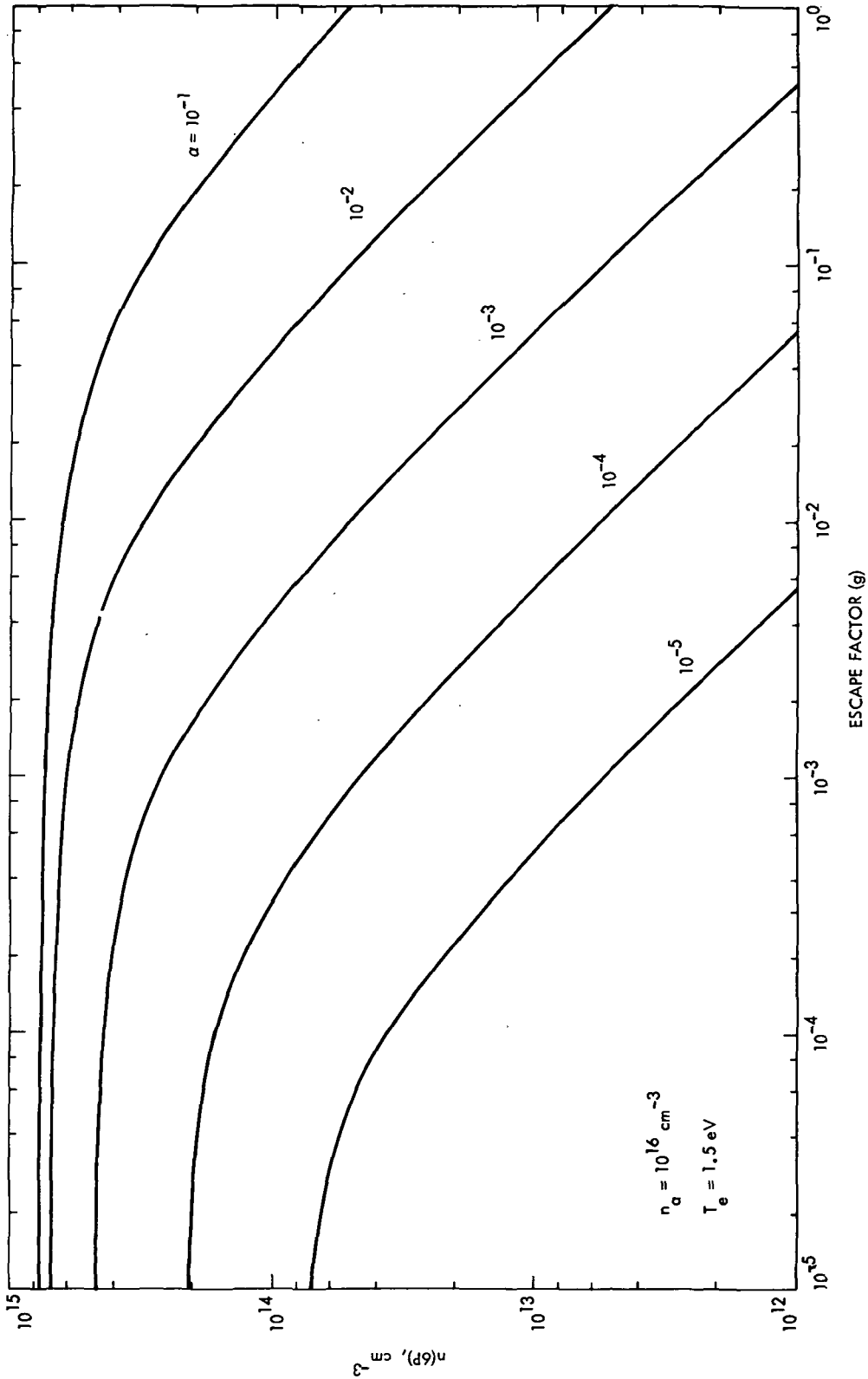


Fig. 10. Dependence of  $n(6P)$  on  $g$ -value for different degrees of ionization at  $n_a = 10^{16} \text{ cm}^{-3}$ ,  $T_e = 1.5 \text{ eV}$